



Synthesis, crystal structure and biological evaluation of a main group seven-coordinated bismuth(III) complex with 2-acetylpyridine N⁴-phenylthiosemicarbazone

Yan-Ke Li^a, Min Yang^a, Ming-Xue Li^{a,*}, Han Yu^a, He-Chen Wu^a, Song-Qiang Xie^{b,*}

^a Henan Key Laboratory of Polyoxometalates, College of Chemistry and Chemical Engineering, Henan University, Kaifeng 475004, PR China

^b Institute of Chemical Biology, Henan University, Kaifeng 475004, PR China

ARTICLE INFO

Article history:

Received 8 January 2013

Revised 18 February 2013

Accepted 21 February 2013

Available online 1 March 2013

Keywords:

Thiosemicarbazone

Bismuth(III)

Crystal structure

Cytotoxicity

Apoptosis

ABSTRACT

Up to now, bismuth(III) complexes with thiosemicarbazones have been comparatively rare. Here, a main group seven-coordinated bismuth(III) complex $[\text{Bi}(\text{L})(\text{NO}_3)_2(\text{CH}_3\text{CH}_2\text{OH})]$ (**1**) (HL = 2-acetylpyridine N⁴-phenylthiosemicarbazone) has been synthesized and characterized by elemental analysis, IR, ¹H NMR and single-crystal X-ray diffraction studies. The cytotoxicity data suggest that **1** exhibits higher in vitro anti-proliferative activity in four human cancer cells tested. Its possible apoptotic mechanism has been evaluated in HepG2 cells. Compound **1** promotes a dose-dependent apoptosis in HepG2 cells and the apoptosis is associated with an increase in intracellular reactive oxygen species (ROS) production and reduction of mitochondrial membrane potential (MMP).

© 2013 Elsevier Ltd. All rights reserved.

Heterocyclic thiosemicarbazones and their metal complexes have received considerable attention in chemistry and biology, primarily because of their marked and different biological properties.¹⁴ It has been reported that biological activities of the thiosemicarbazones are closely related to the parent aldehyde or ketone group, metal chelation ability and amino-terminal substitution.⁵ The biological properties of thiosemicarbazones by the linkage to metal ions can be modified and differ from those of either the ligand or the metal ion itself.^{6–9} In some cases the highest activity is associated with a metal complex rather than the parent ligand and some side effects may decrease upon complexation.^{10,11}

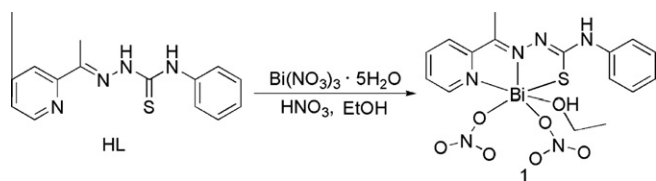
Bismuth(III) compounds have been widely used in the clinic for centuries because of their high effectiveness and low toxicity in the treatment of a variety of microbial infections, including syphilis, diarrhea, gastritis and colitis.^{12–15} Apart from antimicrobial activity, bismuth compounds exhibit anticancer and antiviral activities.^{212Bi and 213Bi compounds have also been used as targeted radio-therapeutic agents for cancer treatment.^{16–23} Furthermore, bismuth(III) ion with a larger ionic radius (1.16 Å) has one inert electron pair (6s²) and forms the complexes with higher coordination numbers which makes their structural characterization interesting and meaningful.}

* Corresponding authors. Tel./fax: +86 378 3881589.

E-mail addresses: limingxue@henu.edu.cn (M.-X. Li), kfxsq@yahoo.com.cn (S.-Q. Xie).

In recent years we have been working on the structural and biological properties of heterocyclic thiosemicarbazones and their transition metal complexes.^{24,25a–c} These results reveal that thiosemicarbazones derived from 2-acetylpyridine and their transition metal complexes show significant cytotoxicity. After a careful literature search, we can affirm that 2-acetylpyridine N⁴-substituted thiosemicarbazones and their bismuth(III) complexes are scarce.^{5,25a–c} One reason may be that the crystals suitable for X-ray diffraction study of these compounds have been difficult to obtain. It is envisaged that they are likely to exhibit interesting properties structurally and biologically. Particularly, information on the mechanism of these compounds is sparse and valuable. Therefore, it seems important for us to obtain their bismuth(III) complexes as a strategy of preparation of new drug candidates in which the metal and ligand could act synergistically.

As a part of our ongoing studies, in the present Letter, we have synthesized and characterized a main group seven-coordinated complex $[\text{Bi}(\text{L})(\text{NO}_3)_2(\text{CH}_3\text{CH}_2\text{OH})]$ (**1**), where HL = 2-acetylpyridine N⁴-phenylthiosemicarbazone (Scheme 1). The main aim of this work is to study anticancer activity and possible apoptotic mechanism of **1**. Apoptosis is a common process of programmed cell death and is the focus of current oncology research. Reactive oxygen species (ROS), which are pro-oxidants, play a critical role in regulating cell death.⁵ Therefore, we examine whether ROS are critical mediators of **1**-induced tumor cell death. In addition, effect of **1** on mitochondria membrane potential (MMP) is also studied. In this report, we present evidence that **1** promotes a dose-dependent



Scheme 1. The reaction scheme for the synthesis of **1**.

apoptosis in HepG2 cells and the apoptosis is associated with an increase in intracellular ROS production and reduction of MMP.

The ligand HL has been prepared by refluxing condensation of 2-acetylpyridine and thiosemicarbazide (1:1 molar ratio) with acetic acid as catalyst in methanol,²⁶ whereas complex **1** was synthesized by reacting 2-acetylpyridine *N*(4)-phenylthiosemicarbazone and $\text{Bi}(\text{NO}_3)_3 \cdot 5\text{H}_2\text{O}$ (1:1 ligand–metal molar ratio) in methanol.²⁷

Single-crystal X-ray analysis reveals that **1** crystallizes in monoclinic system, with space group $P2_1/c$. As shown in Figure 1,²⁸ the molecular structure of **1** is depicted as a monomeric, seven-coordinated complex formed with one electron pair ($6s^2$) of the bismuth(III) ion (Fig. 1A), two nitrogen and one sulfur atoms from one tridentate N_2S thiosemicarbazone ligand and three oxygen atoms from two nitrate ions and one ethanol molecule. The O(3) atom was coordinated to the bismuth(III) ion from one side of the plane formed by S(1), N(3), N(4), O(7) and an electron pair (the sum of $\text{N}(3)\text{--Bi}(1)\text{--N}(4)$, $\text{N}(3)\text{--Bi}(1)\text{--S}(1)$, $\text{S}(1)\text{--Bi}(1)\text{--O}(7)$ and $\text{N}(4)\text{--Bi}(1)\text{--O}(7)$ is 353.15°), while the O(4) atom was coordinated from the opposite side. The bond distances around the bismuth(III) ion ($\text{Bi}(1)\text{--S}(1)$ 2.585(2), $\text{Bi}(1)\text{--N}(3)$ 2.392(1), $\text{Bi}(1)\text{--N}(4)$ 2.484(1), $\text{Bi}(1)\text{--O}(3)$ 2.444(1), $\text{Bi}(1)\text{--O}(4)$ 2.362(1), $\text{Bi}(1)\text{--O}(7)$ 2.712(1) Å) are compared with other data in related bismuth(III) complexes.^{24c,25a–c,29} The longer Bi–N bonds and Bi–S bond are resulting from the larger ionic radius of Bi^{3+} compared to that of Mn^{2+} , Zn^{2+} and Ni^{2+} , respectively.²⁴ Formation of seven-coordinated structure of the bismuth(III) ion is unusual and interesting.³⁰ The molecules of **1** are held together in the crystal packing through intramolecular and intermolecular hydrogen bonds involving the oxygen atom O(7) of ethanol molecule, the terminal nitrogen N(1) atom, the oxygen atoms O(3) and O(5) of the nitrate ions (Fig. 1B). The O(7) and N(1) act as hydrogen bond donors, while the O(3) and O(5) act as acceptors. The separation for $\text{N}(1)\cdots\text{O}(3)$ (symmetry code: $x, y-1, z$) is 3.181(5) Å with the $\text{N--H}\cdots\text{O}$ angle being 143.1° and the separation for $\text{O}(7)\cdots\text{O}(5)$ is 3.247(6) Å with the $\text{O--H}\cdots\text{O}$ angle being 154.0° , respectively.

In view of the biological activity of thiosemicarbazones, we firstly have evaluated the ability of the title complex to inhibit cancer cell growth against human leukemia K562 cells.³¹ In our

experiments, IC_{50} values (compound concentration that produces 50% of cell death) in micro molar units were calculated. For comparison purposes the cytotoxicity of cisplatin (*cis*-DDP) and the free ligand as well as the starting compound $\text{Bi}(\text{NO}_3)_3 \cdot 5\text{H}_2\text{O}$ has been evaluated under the same experimental conditions. It is clearly observed that complexation with metal has a synergistic effect on the cytotoxicity (Fig. 2A). The comparison of cytotoxicity indicates that **1** shows much lower IC_{50} value ($5.22 \mu\text{M}$) than both HL ($94.7 \mu\text{M}$) alone and $\text{Bi}(\text{NO}_3)_3 \cdot 5\text{H}_2\text{O}$ ($41.2 \mu\text{M}$)^{24c} alone. Therefore, the chelation of the free ligand with bismuth(III) ion is essential for anticancer activities of **1**. These results are consistent with the cases of many other analogues of thiosemicarbazones.^{5,25a,25b,32} Importantly, it should be emphasized that **1** shows excellent activity similar to that of cisplatin ($1.2 \mu\text{M}$).^{24c} These gratifying results are encouraging its further screening in vitro. Later on, upon further analysis, **1** also exhibits considerable cell growth inhibition activity against human colorectal cancer HCT-116 cells, human cervical carcinoma Hela cells, human liver hepatocellular carcinoma HepG2 cells (Fig. 2B), respectively. Therefore, its further biological evaluation in vivo as well as studies of mechanism of action is necessary.

In order to confirm that the cell death in HepG2 cells is due to apoptosis, the apoptotic effect of **1** has been assessed with acridine orange (AO) and ethylene dibromide (EB) staining.³³ Mitoxantrone is a kind of antibiotic antitumor drugs, used as the reference compound for comparison. Green live cells with normal morphology were observed in control group (Fig. 3A). Green early apoptotic cells with nuclear margination and chromatin condensation were observed after **1** treatment in a dose-dependent manner, while orange later apoptotic cells with fragmented chromatin and apoptotic bodies were seen after the treatment of mitoxantrone (Fig. 3A). Furthermore, the apoptosis percentage of HepG2 cells significantly increases after **1** treatment, compared with untreated cells and mitoxantrone treated cells (Fig. 3B). These data suggested that **1** could induce liver cancer cells apoptosis in vitro.

The intracellular redox levels are important and play a crucial role in driving the cellular apoptosis.^{5,34} A large body of evidence suggests that the intracellular levels of ROS are associated with the cell death processes and the apoptosis is associated with an increase in intracellular production. In this report, the production of ROS was investigated at that time by fluorescence microscope with the use of DCFH-DA.³⁵ An oxidation of the intracellular DCFH to fluorescent DCF was observed in **1**-treated cells as indicated by the mean fluorescence value, which was higher in **1**-treated cells than in untreated cells (Fig. 4). This data confirmed the production of ROS during **1**-induced HepG2 cells apoptosis.

Mitochondria is considered to be a major site of antitumor agents through electron leakage from the electron transport

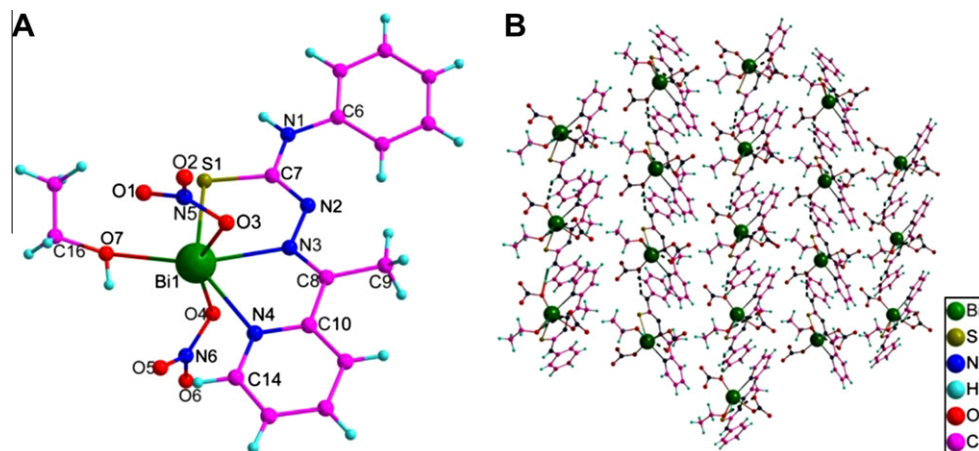


Figure 1. (A) Structure of complex **1** with atomic numbering scheme. (B) Hydrogen bond in dashed lines in complex **1**.

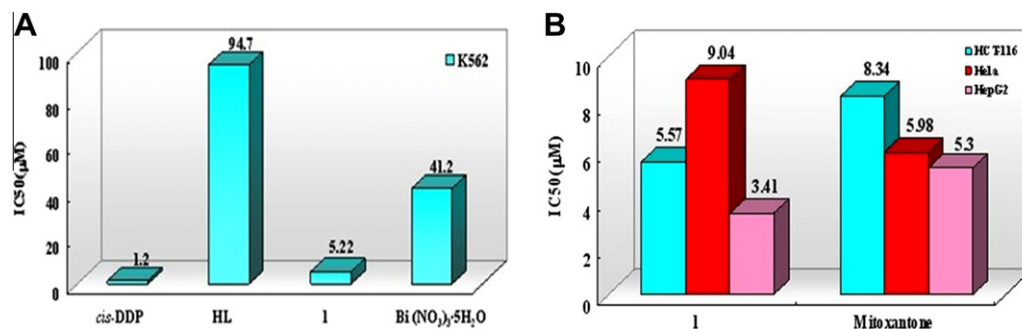


Figure 2. (A) The cytotoxicity of HL and **1** against human leukemia K562 cells. (B) The cytotoxicity of complex **1** on tumor cells. Mitoxantone (Mito) were used as a positive control.

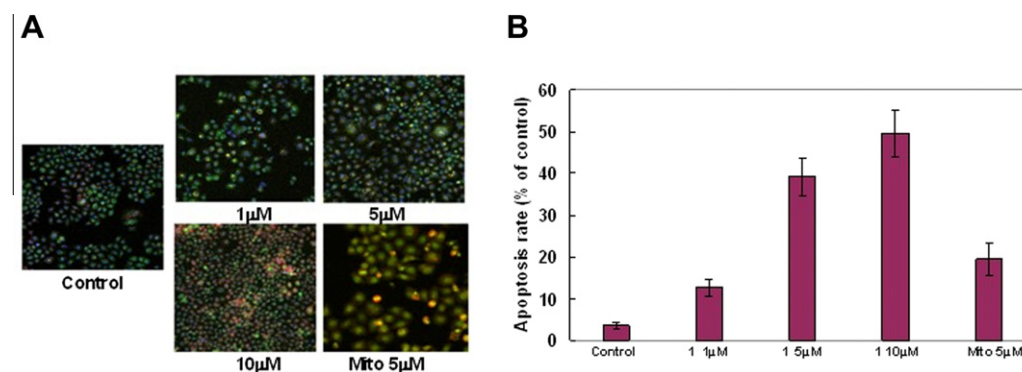


Figure 3. HepG2 cell apoptosis was determined by AO/EB staining with the indicated concentrations of **1** for 48 h. (A) Morphologic observation. (B) Percentages of apoptotic cells were determined using fluorescence microscopy after staining with AO/EB. Mitoxantone (Mito) were used as a positive control.

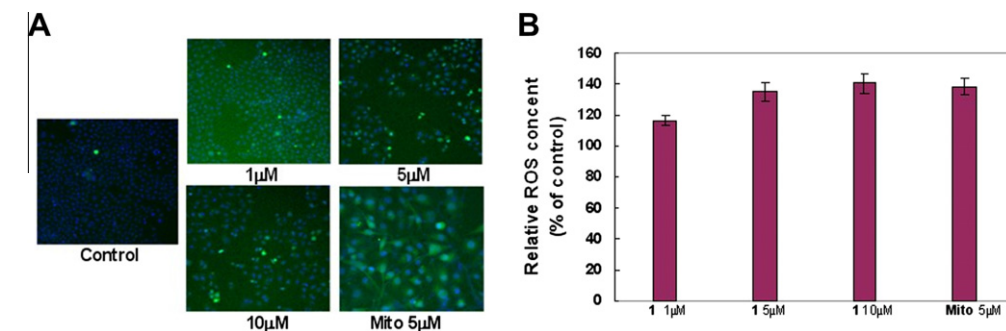


Figure 4. The effects of **1** on intracellular ROS content in HepG2 cells, ($\bar{x} \pm s$, $n = 4$). (A) The representative pictures of ROS generation in **1**-mediated HepG2 cells by DCFH-DA staining. Images were acquired on the ArrayScan® HCS Reader using Cellomics' Target Activation BioApplication. Scale bar = 10 μm. (B) The percentage of ROS in HepG2 cells induced by **1**. Mitoxantone (Mito) were used as a positive control.

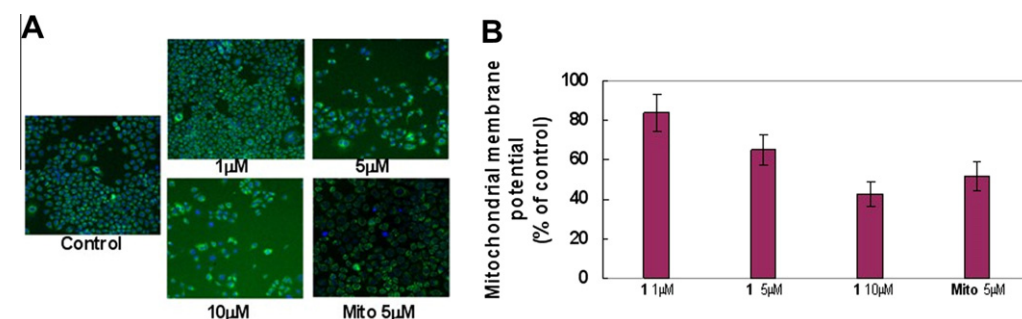


Figure 5. Effect of **1** on MMP in HepG2 cells. (A) The change of MMP was detected by Rh123 and Hoechst 33342 double staining using HCS in HepG2 cells with the indicated concentrations of **1**. (B) Representative pictures are from one of three independent experiments with similar results (magnification, 20×). Each value represents the mean \pm SD ($n = 4$). Mitoxantone (Mito) were used as a positive control.

chain,^{36,37} the decreased MMP may open the mitochondrial permeability transition (MPT) and trigger the release of cytochrome c which activate caspase cascade, causing the cell apoptosis. In the present report, rhodamine 123 (Rh123), a mitochondrial specific stain, which can bind to the inner and outer membrane of mitochondria, and their degrees of fluorescence are proportional to the MMP.³⁸ As shown in Figure 5, the green fluorescence was significant decrease after treatment with **1** for 48 h, suggesting **1** induced the MMP decrease in cells apoptosis.

In summary, the bismuth(III) complex **1** has been synthesized and structurally characterized. It indicates remarkable cytotoxicity and promotes a dose-dependent apoptosis in HepG2 cells and the apoptosis is associated with an increase in intracellular ROS production and reduction of MMP. These promising results are encouraging its further screening in vivo which will provide useful clues in the design of even more effective agents for cancer treatment.

Acknowledgment

This work was financially supported by the National Natural Science Foundation of China (21071043).

Supplementary data

CCDC 851899 contains the supplementary crystallographic data of **1**. These data can be obtained free of charge from the Cambridge Crystallographic Centre via www.ccdc.cam.ac.uk/data_request/cif.

Supplementary data associated with this article can be found, in the online version, at <http://dx.doi.org/10.1016/j.bmcl.2013.02.097>.

References and notes

- Pelosi, G.; Bisceglie, F.; Bignami, F.; Ronzi, P.; Schiavone, P.; Re, M. C.; Casoli, C.; Pilotti, E. *J. Med. Chem.* **2010**, *53*, 8765.
- Beckford, F. A.; Shaloski, M., Jr.; Leblanc, G.; Thessing, J.; Lewis-Alleyne, L. C.; Holder, A. A.; Li, L.; Seeram, N. P. *Dalton Trans.* **2009**, *48*, 10757.
- Padhye, S.; Afrasiabi, Z.; Sinn, E.; Fok, J.; Mehta, K.; Rath, N. *Inorg. Chem.* **2005**, *44*, 1154.
- Kowol, C. R.; Trondl, R.; Heffeter, P.; Arion, V. B.; Jakupc, M. A.; Roller, A.; Galanski, M.; Berger, W.; Keppler, B. K. *J. Med. Chem.* **2009**, *52*, 5032.
- Jansson, P. J.; Sharpe, P. C.; Bernhardt, P. V.; Richardson, D. R. *J. Med. Chem.* **2010**, *53*, 5759.
- Rebolledo, A. P.; Vieites, M.; Gambino, D.; Piro, O. E.; Castellano, E. E.; Zani, C. L.; Souza-Fagundes, E. M.; Teixeira, L. R.; Batista, A. A.; Beraldo, H. *J. Inorg. Biochem.* **2005**, *99*, 698.
- West, D. X.; Bain, G. A.; Butcher, R. J.; Jasinski, J. P.; Li, Y.; Pozdniakiv, R. Y.; Valdés-Martínez, J.; Toscano, R. A.; Hernández-Ortega, S. *Polyhedron* **1996**, *15*, 665.
- Matesanz, A. I.; Pérez, J. M.; Navarro, P.; Moreno, J. M.; Colacio, E.; Souza, P. *Inorg. Biochem.* **1999**, *76*, 29.
- Murafuji, T.; Miyoshi, Y.; Ishibashi, M.; Mustafizur Rahman, A. F.; Sugihara, A. F.; Miyakawa, I.; Uno, H. *J. Inorg. Biochem.* **2004**, *98*, 547.
- Mendes, I. C.; Moreira, J. P.; Ardisson, J. D.; Santos, R. G.; da Silva, P. R. O.; Garcia, I.; Castiñeiras, A.; Beraldo, H. *Eur. J. Med. Chem.* **2008**, *43*, 1454.
- Iakovidou, Z.; Papageorgiou, A.; Demertzis, M.; Mioglou, E.; Mourelatos, D.; Kotsis, A.; Yadav, P. N.; Kovala-Demertzi, D. *Anti-Cancer Drug* **2001**, *12*, 65.
- Suerbaum, S.; Michetti, P. N. *Engl. J. Med.* **2002**, *347*, 1175.
- Briand, G. G.; Burford, N. *Chem. Rev.* **1999**, *30*, 2601.
- Brogan, A. P.; Verghese, J.; Widger, W. R.; Kohn, H. *J. Inorg. Biochem.* **2005**, *99*, 841.
- Kotani, T.; Nagai, D.; Asahi, K.; Suzuki, H.; Yamao, F.; Kataoka, N.; Yagura, T. *Antimicrob. Agents Chemother.* **2005**, *49*, 2729.
- Ge, R.; Sun, H. *Acc. Chem. Res.* **2007**, *40*, 267.
- Li, H.; Sun, H. *Curr. Opin. Chem. Biol.* **2012**, *16*, 74.
- Tiekink, E. R. T. *Crit. Rev. Oncol. Hematol.* **2002**, *42*, 217.
- Yang, N.; Tanner, J. A.; Zheng, B. J.; Watt, R. M.; He, M. L.; Lu, L. Y.; Jiang, J. Q.; Shum, K. T.; Lin, Y. P.; Wong, K. L. *Angew. Chem., Int. Ed.* **2007**, *46*, 6464.
- Yang, N.; Tanner, J. A.; Wang, Z.; Huang, J. D.; Zheng, B. J.; Zhu, N.; Sun, H. *Chem. Commun.* **2007**, *14*, 4413.
- Burke, J. M.; Jurcic, J. G.; Scheinberg, D. A. *Cancer Control* **2002**, *9*, 106.
- McDevitt, M. R.; Finn, R. D.; Ma, D.; Larson, S. M.; Scheinberg, D. A. *J. Nucl. Med.* **1999**, *40*, 1722.
- Kondo, Y.; Himeno, S.; Satoh, M.; Naganuma, A.; Nishimura, T.; Imura, N. *Cancer Chemother. Pharmacol.* **2004**, *53*, 33.
- (a) Li, M. X.; Zhang, D.; Zhang, L. Z.; Niu, J. Y.; Ji, B. S. *Inorg. Chem. Commun.* **2010**, *13*, 1572; (b) Li, M. X.; Chen, C. L.; Zhang, D.; Niu, J. Y.; Ji, B. S. *Eur. J. Med. Chem.* **2010**, *45*, 3169; (c) Zhang, L. Z.; An, G. Y.; Yang, M.; Li, M. X.; Zhu, X. F. *Inorg. Chem. Commun.* **2012**, *20*, 37; (d) Li, M. X.; Zhang, L. Z.; Zhang, D.; Ji, B. S.; Zhao, J. W. *Eur. J. Med. Chem.* **2011**, *46*, 4383; (e) Li, M. X.; Zhang, L. Z.; Chen, C. L.; Niu, J. Y.; Ji, B. S. *J. Inorg. Biochem.* **2012**, *106*, 117.
- (a) Li, M. X.; Yang, M.; Niu, J. Y.; Zhang, L. Z.; Xie, S. Q. *Inorg. Chem.* **2012**, *51*, 12521; (b) Li, M. X.; Lu, Y. L.; Yang, M.; Li, Y. K.; Zhang, L. Z.; Xie, S. Q. *Dalton Trans.* **2012**, *41*, 12882; (c) Li, M. X.; Zhang, L. Z.; Yang, M.; Niu, J. Y.; Zhou, J. *Bioorg. Med. Chem. Lett.* **2012**, *22*, 2418; (d) Näslund, J.; Persson, I.; Sandström, M. *Inorg. Chem.* **2000**, *39*, 4012.
- Synthesis of HL: N(4)-phenyl thiosemicarbazide (0.50 g, 3 mmol) was added dropwise to a methanol solution (30 mL) of 2-acetylpyridine (0.37 g, 3 mmol) with five drops of acetic acid as catalyst. After refluxed for 2 h, the resultant solution was filtered. Yellow powder separated on cooling were washed with methanol and dried over P₂O₅ in vacuo. Yield: 81%-C₁₄H₁₄N₄S (%). Calcd C 62.20, H 5.22, N 20.72. Found C 62.46, H 5.35, N 20.90. mp 182–184 °C. IR (KBr, cm⁻¹): ν(C=N) 1587, ν(N–N) 1189, ν(C=S) 894. ¹H NMR (DMSO-*d*₆, δ ppm): 10.70 (s, 1H, NH), 10.22 (s, 1H, NH), 8.59 (d, *J* = 4.8 Hz, 1H, Py), 8.54 (d, *J* = 8 Hz, 1H, Py), 7.81 (t, *J* = 7.6 Hz, 1H, Py), 7.54 (d, *J* = 8 Hz, 2H, Ph), 7.42–7.31 (m, 2H, Ph), 7.23 (t, *J* = 7.2 Hz, 1H, Ph), 7.15 (t, *J* = 7.2 Hz, 1H, Py), 3.42 (s, 3H, CH₃).
- Synthesis of **1**: Bi(NO₃)₃·5H₂O (0.097 g, 0.2 mmol) solution dissolved in ethanol with the help of a few drops of nitrate acid was added dropwise to an ethanol solution (20 mL) of 2-acetylpyridine N(4)-phenylthiosemicarbazone (0.034 g, 0.2 mmol). After refluxing with stirring for 2 h, the resultant solution was filtered. The solid product formed was recrystallized from ethanol and dried over P₂O₅ in vacuo. Yield: 60%-C₁₆H₁₉BiN₅O₇ (%). Calcd C 29.64, H 2.95, N 12.96. Found C 29.55, H 2.79, N 14.20. mp 212–214 °C. IR (KBr, cm⁻¹): ν(C=N) 1544, ν(N–N) 1258, ν(C=S) 847. ¹H NMR(DMSO-*d*₆, δ ppm): 9.60 (s, 1H, NH), 9.05 (t, *J* = 6 Hz, 1H, Py), 8.29–8.17 (m, 2H, Py), 7.80–7.63 (m, 3H, Ph), 7.39–7.28 (m, 2H, Ph), 7.08–6.97 (m, 1H, Py), 3.43 (s, 3H, CH₃). Orange crystals suitable for X-ray studies were obtained by slow evaporation of its ethanol solution.
- Crystal data for HL: *M* = 648.41, monoclinic, space group *P*2₁/*c*, *a* = 17.962(1) Å, *b* = 7.7290(1) Å, *c* = 17.699(1) Å, *b* = 114.60 (1)°, *V* = 2234.1(7) Å³, *Z* = 2, *D*_c = 1.928 g cm⁻³, *μ* = 8.034 cm⁻¹, *F*(000) = 1248, *T* = 296(2) K. A crystal with approximate dimensions of 0.47 × 0.25 × 0.17 mm³ was mounted on a glass fiber in a random orientation. Crystallographic data were collected with a Siemens Smart-CCD diffractometer with graphite-monochromated MoK_α radiation (*λ* = 0.71073 Å). A total of 11628 reflections was measured by *ω* scan technique at 296(2) K within 2.31 ≤ *θ* ≤ 26.00°, of which 2979 were independent with *R*_{int} = 0.0412, and 4387 were observed with *I* ≥ 2σ (*I*). The structure was solved by Direct Methods and refined by full-matrix least-squares on *F*² with anisotropic displacement parameters for all non-hydrogen atoms using SHELXTL-97 program package. The hydrogen atoms were added in idealized geometrical positions. Final *R* indices [*I* ≥ 2σ (*I*)] : *R*₁ = 0.0292, *wR*₂ = 0.0564.
- Nomiya, K.; Sekino, K.; Ishikawa, M.; Honda, A.; Yokoyama, M.; Kasuga, N. C.; Yokoyama, H.; Nakano, S.; Onodera, K. *J. Inorg. Biochem.* **2004**, *98*, 601.
- Casas, J.; Garcia-Tasende, M.; Sordo, J. *Coord. Chem. Rev.* **2000**, *209*, 197.
- 3-(4,5-Dimethylthiazol-2-yl)-2,5-diphenyltetrazolium bromide (MTT) assay was carried out to evaluate cytotoxicity in K562 cells, HCT-116 cells, Hela cells and HepG2 cells. Cells were plated into 96-well plates at a cell density of 1 × 10⁴ cells per well and allowed to grow in a CO₂ incubator. After 24 h, the medium was removed and replaced by fresh medium containing the tested compounds which were dissolved in DMSO at 0.01 M and diluted to various concentrations with phosphate-buffered saline (PBS) before the experiment. The final concentration of DMSO is lower than 1%. After 24 h incubation, cultures were incubated in 100 μL of medium with 10 μL of 5 mg/mL MTT solution for 4 h at 37 °C. The medium with MTT was removed, and 100 μL of DMSO was added to each well to dissolve the formazan. The absorbance at 570 nm was measured with microplate reader (Bio-Tek ELX800, USA). The inhibitory percentage of each compound at various concentrations was calculated, and the IC₅₀ value was determined.
- Zhang, H.; Thomas, R.; Oupicky, D.; Peng, F. J. *Biol. Inorg. Chem.* **2008**, *13*, 47.
- Cell apoptosis was determined by morphologic observation and Annexin V-FITC. For morphologic observation, cells were stained with acridine orange (AO) and ethylene dibromide (EB) and assessed by fluorescence microscopy. Briefly, 1 μL of a stock solution (100 μg/mL AO and EB) was added to 25 μL of cell suspension. EB-negative cells with nuclear shrinkage, blebbing, and apoptotic bodies were counted as apoptotic cell. The percentage of apoptotic cells was calculated after observing a total of 300 cells. All data were presented as mean ± SD and analyzed using Student's *t*-test or analysis of variance (ANOVA) followed by *q* test. Differences were considered statistically significant at *p* < 0.05.
- Valko, M.; Morris, H.; Cronin, M. *Curr. Med. Chem.* **2005**, *12*, 1161.
- For analysis of intracellular ROS, the oxidation-sensitive fluorescent probe DCFH-DA was used. Cellular fluorescence intensity was measured after 30 min incubation with 10 μM DCFH-DA, using fluorescence microplate reader (Perkin Elmer, USA). All data were presented as mean ± SD and analyzed using Student's *t*-test or analysis of variance (ANOVA) followed by *q* test. Differences were considered statistically significant at *p* < 0.05.
- Turrens, J. F. *J. Physiol.* **2003**, *552*, 335.

37. Lizasoain, I.; Weiner, C. P.; Knowles, R. G.; Moncada, S. *Pediatr. Res.* **1996**, 39, 779.
38. After incubation with **1** with different concentration for 48 h, the HepG2 cells were preloaded with Rh123 (0.25 nM) and Hoechst 33342 (1 μ M) for 30 min at 37 °C, and then rinsed with freshly prepared PBS. The fluorescence intensity

was measured at emission wavelength of 530 nm and excitation wavelengths of 480 nm by High-Content Screening Reader (Array Scan VTI 600, USA). All data were presented as mean \pm SD and analyzed using Student's *t*-test or analysis of variance (ANOVA) followed by *q* test. Differences were considered statistically significant at *p* <0.05.